Materials and Structures (2016) 49:4779–4784
DOI 10.1617/s11527-016-0824-6

ORIGINAL ARTICLE

Shape factors for concrete shrinkage and drying creep in model B4 refined by nonlinear diffusion analysis

Abdullah Dönmez · Zdeněk P. Bažant

Received: 19 May 2015 / Accepted: 4 February 2016 / Published online: 9 February 2016

Abstract The source of shrinkage and drying creep is the drying process. From the diffusion analysis of drying one can estimate the shrinkage strain. Same as drying, the shrinkage times scale as the square of the effective specimen thickness (or size), D, commonly characterized by the volume-surface ratio. But there is also an additional effect of cross section shape. In the creep and shrinkage prediction model B4 (a new Draft RILEM Recommendation, Mater Struct 48:753–750, 2015), the shape effect is taken into account by shape factor k_s multiplying D. However, because of the strong nonlinearity of the diffusion equation for drying, the optimal k_s values depend also on the environmental humidity. In model B4, as well as its predecessors since 1975, the k_s values have been specified for typical shapes, i.e. the slab, cylinder, prism, sphere and cube, with values calculated approximately for only one relative humidity—65 %. Here the k_s values for the same typical shapes are calculated with greater accuracy and for different environmental humidities—30, 40, 50, 60, 70 and 80 %, which allows interpolation in between. The k_s values for the typical shapes range from 1.00 to 1.41.

Keywords Drying · Shrinkage · Creep · Shape effect · Moisture diffusion · Concrete

A. Dönmez
Faculty of Civil Engineering, Istanbul Technical University, Istanbul, Turkey

Z. P. Bažant (✉)
McCormick Institute Professor and W.P. Murphy Professor of Civil and Mechanical Engineering and Materials Science, Northwestern University, 2145 Sheridan Road, CEE/A135, Evanston, IL 60208, USA
e-mail: z-bazant@northwestern.edu

1 Introduction

In model B4, the new RILEM Draft Recommendation on Creep and Shrinkage of Concrete published in 2015 [1–3], the drying times depend on the shape of specimen or cross section. This dependence is characterized by shape factor, k_s, whose values are co-opted from preceding models developed at Northwestern University beginning 1978 (models BP, BPKX and B3) cited in [1]. Originally, the k_s values were approximately calculated in 1976 [5] from the half-time of average pore relative humidity, based on the diagrams obtained in [4] by solving the nonlinear diffusion equation of drying of concrete for one fixed value of environmental humidity, $h = 0.65$ [5]; these values were k_s = 1.00 for an infinite slab, 1.15 for an infinite cylinder, 1.25 for an infinite prism, 1.30 for a sphere, and 1.55 for a cube.

However, the decrease of diffusivity $C(H)$ of concrete with decreasing pore relative humidity, H, [4] makes the diffusion equation highly nonlinear. Consequently, factor k_s must have different values for different environmental humidities. A table of these values is here calculated, to be used as a refinement of model B4.

2 Approximate formula for shrinkage in model B4

The shrinkage of concrete as well as the drying cross effect on creep (called the Pickett effect) is caused by the increase of capillary tension, and by the decreases of disjoining pressure in hindered adsorbed layer and of spreading pressure in free water adsorption layers, with the drop of spreading pressure resulting into an increase of the total solid surface tension on nano-scale globular grains of cement. The diffusion equation for moisture transport governing the pore relative humidity, H, [4] can be formulated in terms of the mass concentration of pore water or in terms of H itself. The latter is preferable since it minimizes the mathematical complications due to pore space change and water sink through cement hydration [4].

The relationship of shrinkage to drying is based on two widely accepted simplifying hypotheses:

1. The drying shrinkage strain of a specimen is approximately proportional to the water loss from the specimen.
2. The isotherm of water loss versus pore relative humidity is approximately linear (it suffices that this hypothesis be good only for desorption, and only for relative humidities $> 30\%$).

Thus the average drying shrinkage strain ϵ_{sh} in a cross section of structural member is considered to be roughly proportional to the average decrease of H in the cross section [2]. The evolution of ϵ_{sh} in a specimen instantly exposed at age t_0 to environmental humidity h is in B4 (as well as B3) described by the following formula derived by matching the asymptotics of the diffusion equation and considering the effect of aging on the terminal asymptotics:

$$\epsilon_{sh} = \epsilon_{s\infty} k_h k_a \tanh \sqrt{\frac{\hat{t}}{\tau_{sh}}} \tag{1}$$

$$\tau_{sh} = k_1 (k_s D)^2 \tag{2}$$

$$D = 2V/S, \quad \hat{t} = t - t_0 \tag{3}$$

$$k_a = \sqrt{0.99 + \frac{4.63}{t_0 + \tau_{sh}}} \tag{4}$$

where t, t_0 is the current time and concrete age at exposure to drying (all times are in days); τ_{sh} is the shrinkage halftime; $D = 2V/S$ is the effective thickness (or size) of the specimen or structural member and V and S are its volume and exposed surface (factor 2 is used to make D equal to the actual thickness when an infinite flat slab is considered); $\epsilon_{s\infty}$ is the final shrinkage strain for reference conditions $h = 0$, $t_0 =$ 7 days and $\tau_{sh} = 600$ days; $k_h = 1 - h^3$ is the empirical correction factor for environmental relative humidity h (if $h < 0.98$); k_1 is the empirical factor depending on concrete strength (dimension days/mm^2); k_a is the age factor (empirical, introducing the effect of concrete age, or degree of hydration up to shrinkage half-time); and k_s is the shape factor (derived by fitting the numerical simulations of the nonlinear diffusion equation).

Since the additional creep due to drying is in model B4 (as well as its predecessor B3) described with the help of the shrinkage function, the same shape factor also controls the effect of cross-section geometry on drying creep.

3 Nonlinear diffusion equation and its solution

The diffusion equation for $H(\boldsymbol{x}, t)$, which underpins Eq. (1) for ϵ_{sh}, is obtained by combining the Darcy's law with the water sorption isotherm which, according to the aforementioned hypothesis, is considered approximately linear during drying. It has the form:

$$\frac{\partial H}{\partial t} = \nabla [C(H) \nabla H] \tag{5}$$

where t is the time, $\boldsymbol{x}$ is the spatial coordinate vector; C is the diffusivity which, according to measurements [4], depends on H as follows:

$$C(H) = C_1 \left(\alpha_0 + \frac{1 - \alpha_0}{1 + \left(\frac{1-h}{1-h_c} \right)^n} \right) \tag{6}$$

where C_1 is the diffusivity at saturation (as an average, C_1 is considered as 30 mm^2/day but can vary by orders of magnitude among different concretes); α_0 is the dimensionless empirical ratio of diffusivity at low humidity to diffusivity at saturation, with the typical value of 0.05; h_c is the humidity at the center of the transition between low and high diffusivity (typically 0.8); n is the dimensionless exponent (a high value of n, typically 12, is needed to describe the rapid transition between high and low diffusivity).

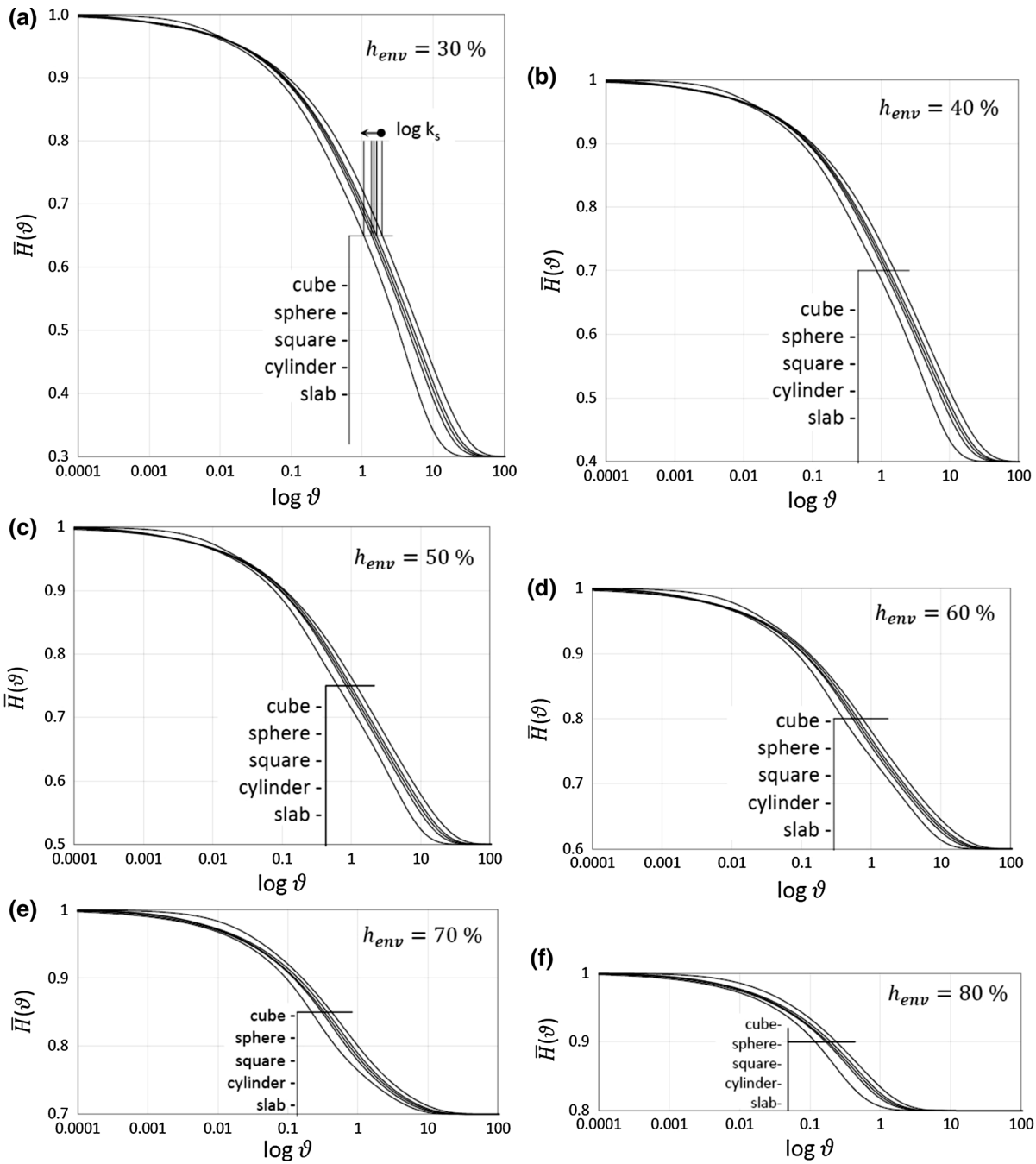

Fig. 1 **a–f** Drying concrete specimens exposed to different environmental humidities, h_{env}. Average cross sectional (or average volume) pore relative humidities, $\bar{H}(\vartheta)$, versus dimensionless time, ϑ, plots

Equation (6) has been verified and calibrated in [4] by the classical measurements reported in [9–15]. Here this equation is solved numerically for the boundary conditions $H = h$ (for all $t \geq t_0$) with various constant values of h, and the initial condition of $H = 1$ for all $\boldsymbol{x}$. Because of the D^2 scaling of drying times, it suffices to do the numerical calculations in terms of dimensionless time and dimensionless coordinate vector:

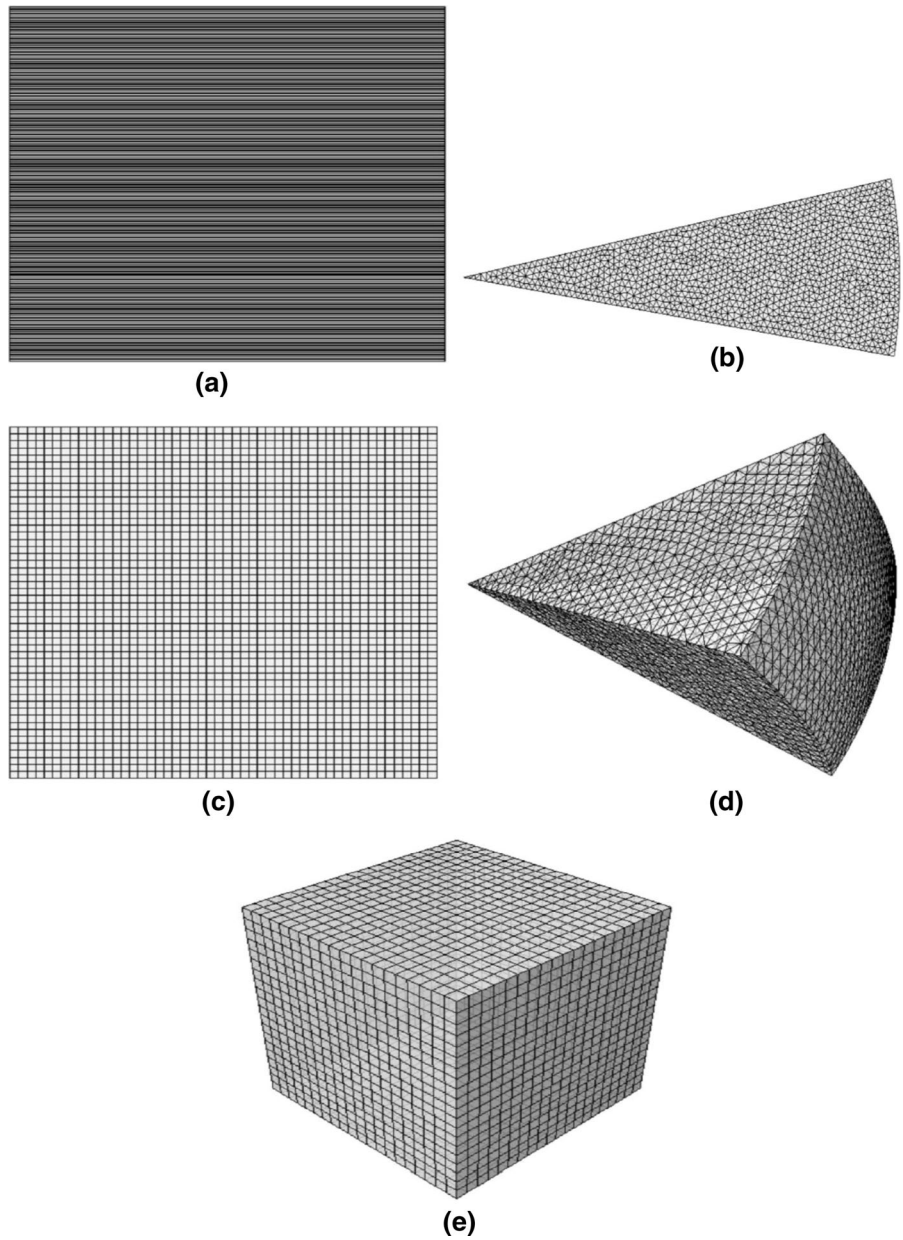

Fig. 2 Mesh discretizations: **a** subdivision across the thickness of *slab*, **b** sliced part of *cylinder*, **c** one quarter part of *square prism*, **d** sliced part of *sphere*, **e** 1/8 part of *cube*

$$\vartheta = \frac{\hat{t}}{k_1 D^2}, \quad \boldsymbol{\xi} = \frac{\boldsymbol{x}}{D} \tag{7}$$

Here the shape factor, k_s, cannot be included in the dimensionless time because its values are what needs to be found.

The numerical solution furnished the spatial profiles of $H(\boldsymbol{\xi}, \vartheta)$ at subsequent discrete times ϑ. From these, the average values $\bar{H}(\vartheta)$ of $H(\boldsymbol{\xi}, \vartheta)$ over the cross section area or volume of specimen have been computed for subsequent dimensionless times ϑ; see Fig. 1a–f. The axisymmetry and spherical symmetry have, of course, been taken into account in calculating the averages. The slab and square prism were discretized with linear quadrilateral elements, the cylinder with linear triangular elements, the sphere with linear tetrahedral elements and the cube with linear hexahedral elements. The mesh fineness was chosen after trying various degrees of mesh

Table 1 Shape factors of specimen shapes for different environmental humidities

h_{env} (%)	Slab	Cylinder	Square	Sphere	Cube
30	1.00	1.13	1.17	1.23	1.34
40	1.00	1.13	1.18	1.24	1.35
50	1.00	1.14	1.20	1.26	1.36
60	1.00	1.18	1.22	1.28	1.39
70	1.00	1.18	1.23	1.28	1.40
80	1.00	1.19	1.24	1.30	1.41

refinement. The meshes are shown in Fig. 2a–e. For all shapes, they were uniform in order to keep the averages unaffected from computational errors

From these results, the average dimensionless humidity half-times, τ_H, defined as the dimensionless time required for $\bar{H}$ to drop half-way toward the final equilibrium value, i.e., to $H_\tau = (1 + h)/2$, have been computed for various simple cross section shapes, with the infinite slab chosen as the reference case, denoted as $\tau_{H,\text{ref}}$. The shape factor for each shape is then calculated as

$$k_s^2 = \tau_H \,/\, \tau_{H,\text{ref}} \tag{8}$$

In the logarithmic time scale plot, it means that the shrinkage evolution curve for a given shape is at the half-time points shifted by $\log k_s$ ahead of the reference curve (a slab); see Fig. 1a–f showing the computed diagrams for 6 different environmental humidities. The five curves in each diagram are the shrinkage evolution curves for an infinite slab, infinite cylinder, infinite square prism, a sphere and a cube (note that, e.g., a finite length cylinder with sealed ends is equivalent to an infinite cylinder). The improved shape factors are given in Table 1. The differences from the 5 values of k_s in [1] are neither large nor negligible.

Note that, to obtain k_s, the calculations could also be done in real rather than dimensionless time, because factors D^2 in the halftimes in Eq. (8) would cancel out. But then Fig. 1 would not have general validity for any D.

4 Closing remarks

Aside from the calculation of shrinkage effects in structures, knowing the correct shape factor is important for extrapolating short-time shrinkage and drying creep data to long times. One of the two shrinkage extrapolation methods described in [8], namely the size effect method, uses specimens that differ by both size and shape, and thus depend on having an accurate value of k_s.

The autogenous shrinkage does not belong into k_s. If important, it can be approximately taken into account by the B4 model formulas. Likewise for self-desiccation, which is the cause of autogenous shrinkage. Anyway, the self-desiccation and temperature change due to hydration cannot be included in the shape factor k_s. To take them more accurately into account, a more complicated formulation with additional factors would be needed. However, for most situations these effects do not seem to make much difference.

Acknowledgments Partial financial support has been obtained under grant CMMI-1129449 of the U.S. National Science Foundation. The first author thanks The Scientific and Technological Research Council of Turkey for financially supporting his pre-doctoral fellowship at Northwestern University.

References

1. Technical Committee RILEM, TC-242-MDC (Z.P. Bažant, chair), (2015) Model B4 for creep, drying shrinkage and autogenous shrinkage of normal and high-strength concretes with multi-decade applicability. (RILEM draft recommendation: TC-242-MDC multidecade creep and shrinkage of concrete: material model and structural analysis). Mater Struct 48:753–750
2. Hubler MH, Wendner R, Bažant ZP (2015) Statistical justification of model B4 for drying and autogenous shrinkage of concrete and comparisons to other models. Mater Struct 48:797–814
3. Wendner R, Hubler MH, Bažant ZP (2015) Statistical justification of model B4 for multi-decade concrete creep using laboratory and bridge databases and comparisons to other models. Mater Struct 48:815–833
4. Bažant ZP, Najjar LJ (1972) Nonlinear water diffusion in nonsaturated concrete. Mater Struct (RILEM, Paris) 5:3–20
5. Bažant ZP, Osman E, Thonguthai W (1976) Practical formulation of shrinkage and creep in concrete. Mater Struct RILEM 9:395–406
6. Bažant ZP, Baweja S (1995) Justification and refinement of Model B3 for concrete creep and shrinkage. 2. Updating and theoretical basis. Mater Struct (RILEM, Paris) 28:488–495
7. Bažant ZP, Baweja S (2000) Creep and shrinkage prediction model for analysis and design of concrete structures: Model B3. In: Al-Manaseer A (ed.) Adam Neville symposium: creep and shrinkage-structural design effects, ACI SP-194.

American Concrete Institute, Farmington Hills, Michigan, pp 1–83 (minor update of [6])
8. Bažant ZP, Donmez A (2015) Extrapolation of short-time drying shrinkage tests based on measured diffusion size effect: concept and reality. Mater Struct (RILEM) 49(1):411–420
9. Abrams MS, Gustaferro AH (1968) Fire endurance of concrete slabs as influenced by thickness, aggregate type, and moisture. J Portland Cem Assoc Res Dev Lab 10(2):9–24 (PCA Bulletin 223)
10. Abrams MS, Monfore GE (1965) Application of a small probe-type relative humidity gage to research on fire resistance of concrete. J Portland Cem Assoc Res Dev Lab 7(3):2–12 (PCA Bulletin 186)
11. Abrams MS, Orals DL (1965) Concrete drying methods and their effect on fire resistance, in: Moisture of materials in relation to fire tests. STP No. 385:52–73, publ. by American Society for Testing Materials (PCA Bulletin 181)
12. Hancox NL (1967) A note on the form of the rate of drying curve for cement paste and its use in analyzing the drying behavior of this material. RILEM Bull 36:197–201
13. Hanson JA (1968) Effects of curing and drying environments on splitting tensile strength. Am Concr Inst J 65:535–543 (PC A Bulletin D141)
14. Helmuth RA, Turk DH (1967) The reversible and irreversible drying shrinkage of hardened portland cement and tricalcium silicate paste. J Portland Cem Assoc Res Dev Lab 9(2):8–21 (PCA Bulletin 215)
15. Hughes BP, Lowe IRG, Walker J (1966) The diffusion of water in concrete at temperatures between 50 and 95 ° C. Br J Appl Phys 17:1545–1552